Study of 2D Materials by a Time-of-Flight Spectrometer for Low-Energy Electrons

I. KONVALINA, B. DANIEL, M. ZOUHAR, A. PATÁK, L. PRŮCHA, J. PIŇOS, I. MÜLLEROVÁ, E. MATERNA MIKMEKOVÁ

Institute of Scientific Instruments of the CAS, v. v. i.,
Department of Electron Microscopy, Královopolská 147,
CZ 612 64 Brno, Czech Republic
e-mail: konvalina@isibrno.cz

ABSTRACT

Theoretical and experimental studies of low and medium energy electron transport near solid surfaces are important for surface sensitive electron spectroscopy and microscopy. Particularly, in order to obtain quantitative information, it is necessary to have a reliable knowledge of electron transport in the sample and across its interface(s). The small thickness of 2D materials motivated us to develop a unique device analyzing samples via transmitted electrons in a standard microscopic regime and also via time-of-flight (ToF) spectroscopic method [1].

UHV SLEEM/ToF SYSTEM - EXPERIMENTAL SETUP

The ultra-high vacuum (UHV) scanning low energy electron microscope (SLEEM) equipped with ToF spectrometer (Figure 1) was developed and assembled at the Institute of Scientific Instruments (ISI). The UHV SLEEM/ToF system can operate as a standard scanning electron microscope in the range of primary beam energy from 5 keV to units of eV. The microscope is equipped with an electron gun developed by Delong Instruments [2], an in-house built specimen manipulator with biased sample holder for use of the cathode lens (CL) mode [3], and several electron detectors for secondary, backscattered and transmitted electrons.

Detectors

In-lens: - integral (SE)
- energy spectral (SE + BSE)

Out-lens: - BSE detector (SE + BSE)
- TimePix 2D (TE)

ToF spectrometer: - MCP (TE)

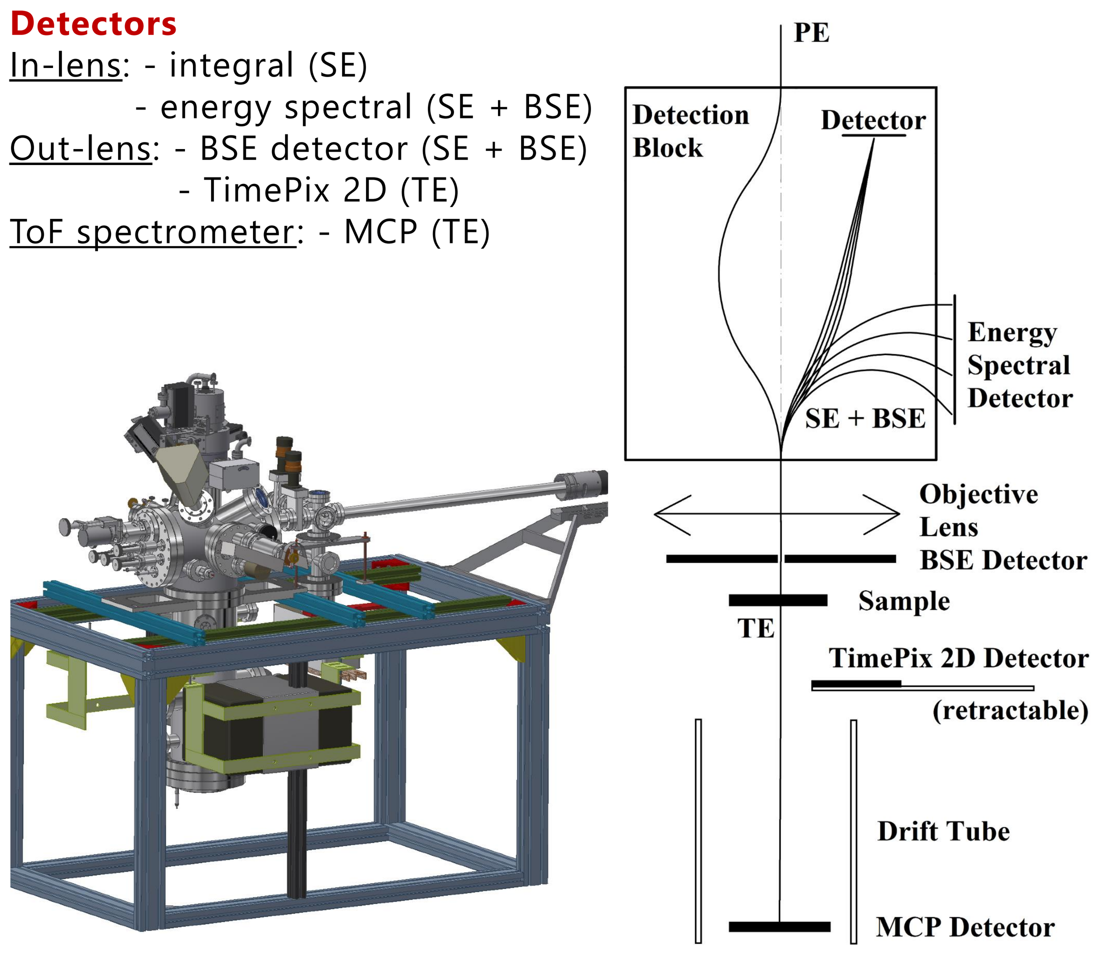

Fig. 1. UHV SLEEM/ToF tool (left); arrangement scheme (right). ToF spectrometer inserted to below the sample for TEs detection.

DISPLAYING AND VIEWING DATA

The new operating mode, the ToF mode, allow us to measure the ToF spectra [4] of electrons transmitted through the sample. The commercial electronics provided with the multi-channel plate (MCP) detector [5] has been complemented by other components.

This includes a pulse generator which allows the microscope to work in a pulse mode enabling the ToF spectrometer functionality. The software supplied to the MCP detector records timestamps of all three types of events, namely signal detections at the MCP, pulse emission towards a given pixel of the sample and pixel switch. These timestamps are used to reconstruct the image of the sample (Figure 2 displaying grayscale intensity of detections for each pixel).

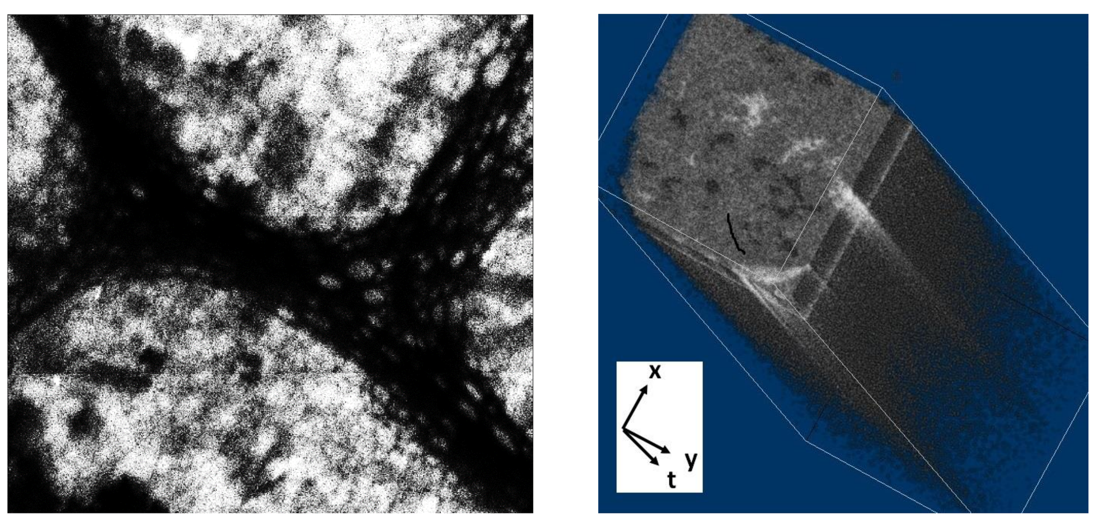

Fig. 2. Transmission image of graphene sample taken by the MCP detector (left). Visualization of the 3D hyperspectral data, the pixel sliced time-domain histogram collected over all frames (right).

ANALYSIS OF HYPERSPECTRAL DATA FOR 3-5 LAYER GRAPHENE

We have performed many experiments for 3-5 layer graphene [6]. Preliminary results are presented in this poster. A useful way to analyze the hyperspectral data is to split them into components, using methods such as principal component analysis (PCA) [7]. An example of such a component split is provided in Figure 3. This processing is done with the intention of finding areas with different spectra, e.g. due to different thickness. Further processing is done using masks created with help of the component-split images. We use at least 3 components in the PCA analysis. This number covers the expected number of layers of the sample.

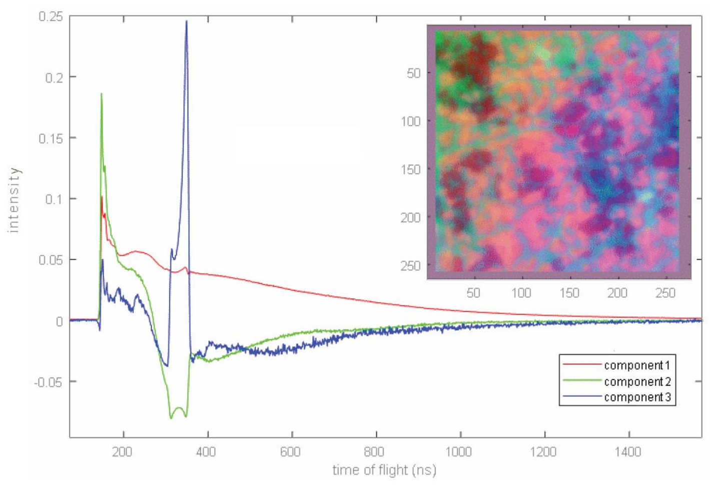

Fig. 3. The first three PCA components of data. Colors of the inset image are PCA coefficients scaled to fit between 0 and 1 to fully utilize the available color range. Note that the color of the area removed by mask used, to filter out region of inferior quality on the sample, corresponds to coefficient of value 0.

GRAPHENE CLEANING BY SLOW ELECTRONS

The cleaning effect of slow electrons on graphene was already known [8], but has not been investigated using electron spectroscopy. 3-5 layer graphene was used. An area of 25 x 25 µm was measured and subsequently cleaned with slow electrons of landing energy of 50 eV for 14 hours (see Figure 4). The energy spectra from the same area of the sample after cleaning are shown in Figure 5.

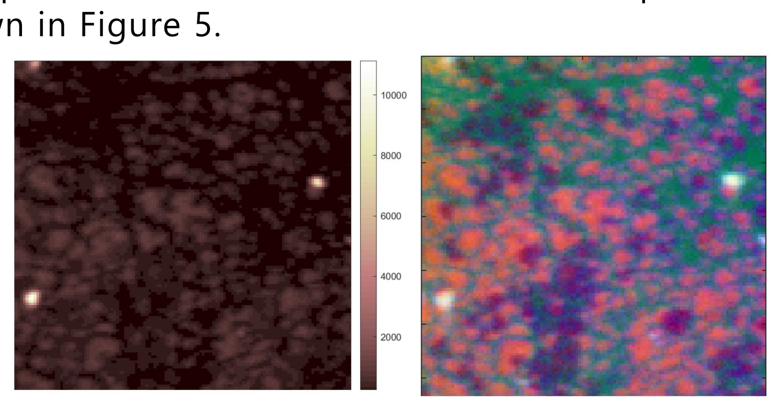

Fig. 4. Intensity (left) and PCA (right) images after cleaning by low energy electrons.

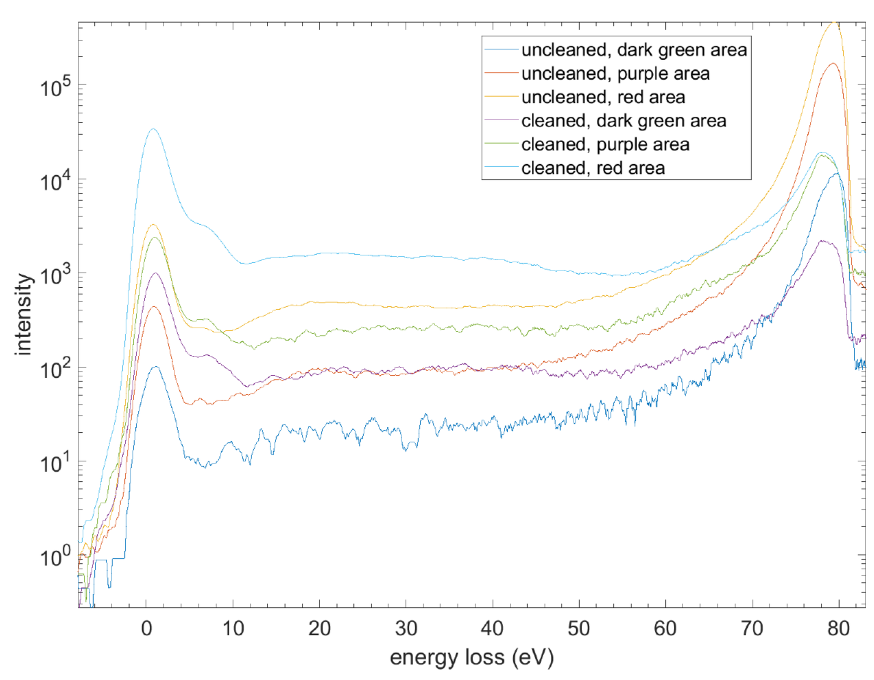

Fig. 5. Spectra before ("uncleaned") and after ("cleaned") cleaning by slow electrons. The colors used in the labels refer to the colors of the PCA image on the right side of Figure 4. The thickness of each colored area could not be confirmed independently, but given the 3-5 layered nature of the sample, a thickness of 3 (red), 4 (purple) and 5 (dark green) layers is assumed. The landing energy was 80 eV, thus the peak near 80 eV loss is from SEs.

PLASMON MEASUREMENTS

For the plasmon measurement, the sample was split into areas assumed to correspond to two to five layers. The determined areas are shown in Figure 6.

The experiment was performed for the 3-5 layer sample using the following method: First, the frame was investigated and split into different suspected thickness areas using PCA. The results were used to create mask of each thickness (including the small suspected 2 layer area), and another mask for the hole.

We utilise the PCA analysis in other measurements on the same sample as well, this time with landing energy 300 eV.

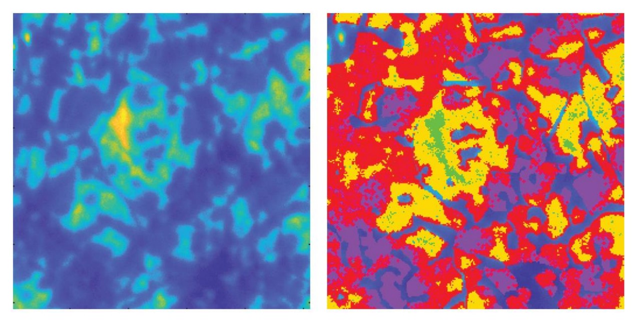

Fig. 6. Intensity image of the 3-5 layer sample (left) and same image with masks overlaid (right). The component masks are assumed to correspond to thicknesses of 2 (green), 3 (yellow), 4 (red) and 5 (purple) layers of graphene.

The energy spectra of the different areas appear rather similar, with the most notable difference being overall intensity, as shown in Figure 7. The π plasmon peak can be clearly seen around 5.8 eV, while the π +σ plasmon peak is much weaker and broader, between approx. 14 and 21 eV loss. Their position shift to higher losses with increasing assigned number of layers which confirms such a labelling.

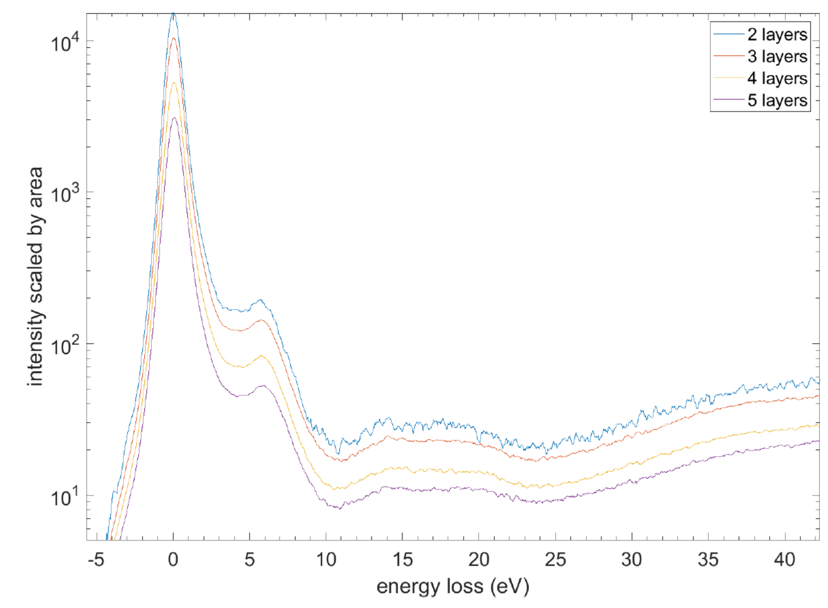

Fig. 7. Spectra of the masks displayed in Figure 6, scaled by area. There are clear differences in intensity between the masks. Note that the number of layers has not been independently confirmed.

CONCLUSION

Matlab scripts allow sufficiently fast processing of the data and semi-automatic correction of problematic data and drift works well.

The resulting hyperspectral images can be simplified and viewed in several ways, from simple intensity images and integrated spectra, over selection of areas using masks and component-splitting via PCA, to viewing the full 3D data cube using, e.g. FIJI.

The obtained energy-loss spectra for graphene are in reasonable agreement with the available literature. The overall shape of the spectrum contains both expected loss-features, the two plasmon peaks. The π plasmon peaks are fairly close to experimental values presented in [9] though they exhibit an inconsistent shift up to 0.25 eV (compared with their q = 0 Å^{-1}). The presumable 5 layers to lower position (which would correspond to negative q) while the 2 layers to higher losses (indicating q = 0.4 Å^{-1}).

The shift to higher values is expected to be a natural consequence of the non-zero momentum transfer (MT) q being collected in our measurements. The data in Ref. [9] indicate that the 5-layer graphene is the most sensitive to uncertainty in MT and Δq ~ 0.02 Å^{-1} can already produce such a shift. Unfortunately, their data show no MT error or error-bars in the π plasmon dispersion relations to make a more realistic comparison.

Thus, we conclude that the PCA component analysis presented here provides components seemingly corresponding well to the different graphene layers though a refinement may be needed.

REFERENCES:

[1] I. Konvalina, et al., Nanomaterials 11 (2021) 2435.
[2] DIGUN, https://www.delong.cz/products/electron-guns/ (accessed September 20, 2022).
[3] I. Müllerová and L. Frank, Adv. Imag. Elect. Phys. 128 (2003), p. 309-443.
[4] W.E. Stephens, Phys. Rev. 69 (1946), p. 691.
[5] RoentDek Delayline Detectors, www.roentdek.com/detectors/ (accessed SEptember 20, 2022).
[6] https://www.tedpella.com/ (accessed September 20, 2022).
[7] K. Pearson, Philosophical Magazine 2 (1901), p. 559-572.
[8] E.M. Mikmeková, et al., J. Electron Spectrosc. Relat. Phenom. 241 (2020) 146873.
[9] P. Wachsmuth, et al., Phys. Rev. B 90 (2014) 235434.

T A Č R
Technology Agency of the Czech Republic

CE PO
Centre of Electron and Photonic Optics

ACKNOWLEDGMENTS:
The research was financially supported by the Technology Agency of Czech Republic project No TN01000008.

CONTACT: Ivo Konvalina
konvalina@isibrno.cz